

# Anomalous X-ray Scattering Study of GeO<sub>2</sub> Glass

E. Matsubara, K. Harada, and Y. Waseda

Research Institute of Mineral Dressing and Metallurgy (SENKEN),  
Tohoku University, Sendai, 980 Japan

M. Iwase

Department of Metallurgy, Faculty of Engineering, Kyoto University, Kyoto, 606 Japan

Z. Naturforsch. **43a**, 181–186 (1988); received November 16, 1987

The anomalous X-ray scattering (AXS) technique was applied to a structural study of GeO<sub>2</sub> glass, using synchrotron radiation and a new goniometer system. The environmental radial distribution function (RDF) was determined from intensity measurements at the Ge K absorption edge and compared with the ordinary RDF curve estimated from the X-ray scattering intensity by Mo K  $\alpha$  radiation. By combining the environmental and ordinary RDFs of the GeO<sub>2</sub> glass it has been confirmed that the fundamental local unit structure is a GeO<sub>4</sub> tetrahedron and that these tetrahedra are joined at their corners to form a network structure. The capability of the AXS technique has been approved as a relatively new tool for the structural characterization of disordered materials.

## Introduction

Germanate (GeO<sub>2</sub>) glass is believed to have an atomic structure similar to silicate (SiO<sub>2</sub>) glass, although there have been rather few structural studies. Lorch [1] found in studies of GeO<sub>2</sub> glass by neutron diffraction that the coordination number of oxygen around germanium calculated from the area under the first peak in the radial distribution function (RDF) is 3.8 and concluded that GeO<sub>4</sub> tetrahedra are the fundamental local unit structures. This conclusion was supported by a time of flight neutron diffraction study [2]. Bondot [3] tried to determine the RDFs of the Ge–O, Ge–Ge and O–O pairs from the three independent scattering profiles of a GeO<sub>2</sub> glass obtained with Cu K  $\alpha$  and Ag K  $\alpha$  radiations, and neutrons. However, his results suffer from the rather limited experimental accuracy at that time (1974).

For these reasons, the anomalous X-ray scattering (AXS) technique was applied to GeO<sub>2</sub> glass at the Ge K absorption edge, and then an environmental structure around a Ge atom was determined and compared with the conventional X-ray diffraction results of Mo K  $\alpha$  radiation. The AXS measurements were carried out using a goniometer system exclusively built for the present purpose using synchrotron radiation in the Photon Factory (PF) of the National Labo-

ratory for High-Energy Physics, Tsukuba, Japan. The main purpose of this paper is to present new structural information on GeO<sub>2</sub> glass, together with a brief description of our AXS system and the essential points of data analysis for the AXS measurements of disordered materials.

## Experimental and Data Analysis

The GeO<sub>2</sub> glass sample was prepared by melting germanium dioxide powder (99.999%) in a shallow platinum dish in air for about 600 sec at 1773 K, followed by furnace-cooling. The obtained sample was about 30 mm in diameter and a few mm thick. Scattering from the Pt dish was not observed because the sample was thick enough for the energy region employed.

A beam line (7C station) in the PF of Tsukuba, Japan, where a double Si 111 crystal monochromator is provided upstream, was used for the present AXS measurements. Any energy of the incident beam from 4 to 20 keV could be selected with this monochromator. Its optimum energy resolution is about 7 eV at 10 keV. The beam from the monochromator can be sagittally focused by bending the second crystal, which is a diamond-shape Si crystal cut with stiffening ribs to prevent antielastic bending [4] in order to increase the power of the incident beam. The fluxes of the incident beam to the sample are of the order of 10<sup>9</sup>

Reprint requests to Dr. E. Matsubara, Research Institute of Mineral Dressing, and Metallurgy (SENKEN), Tohoku University, Sendai 980, Japan.

0932-0784 / 88 / 0200-0181 \$ 01.30/0. – Please order a reprint rather than making your own copy.



Dieses Werk wurde im Jahr 2013 vom Verlag Zeitschrift für Naturforschung in Zusammenarbeit mit der Max-Planck-Gesellschaft zur Förderung der Wissenschaften e.V. digitalisiert und unter folgender Lizenz veröffentlicht: Creative Commons Namensnennung-Keine Bearbeitung 3.0 Deutschland Lizenz.

Zum 01.01.2015 ist eine Anpassung der Lizenzbedingungen (Entfall der Creative Commons Lizenzbedingung „Keine Bearbeitung“) beabsichtigt, um eine Nachnutzung auch im Rahmen zukünftiger wissenschaftlicher Nutzungsformen zu ermöglichen.

This work has been digitalized and published in 2013 by Verlag Zeitschrift für Naturforschung in cooperation with the Max Planck Society for the Advancement of Science under a Creative Commons Attribution-NoDerivs 3.0 Germany License.

On 01.01.2015 it is planned to change the License Conditions (the removal of the Creative Commons License condition “no derivative works”). This is to allow reuse in the area of future scientific usage.

photons/sec without focusing the beam. A detailed documentation about the beam line including this monochromator is available in [5].

An  $\omega$ - $2\theta$  double-axis goniometer, originally designed for precision diffractometry and topography by Ishikawa *et al.* [6], was modified so as to mount a handy intrinsic pure Ge solid state detector, and receiving and scatter slits. Both axes are independently driven by stepping motors with  $0.0002^\circ$  for the  $\omega$  axis and  $0.0004^\circ$  for the  $2\theta$  axis in each step. Since the synchrotron radiation is completely polarized in the orbital plane of the electrons, the goniometer must be placed vertically in order to avoid the polarization effect. For this purpose, the goniometer is mounted on a translation table along the horizontal and vertical directions with 0.002 mm in each step in order to adjust the sample position for alignment of the goniometer. By using coil springs attached to the goniometer and the table, the vertical translation can be smoothly carried out. Also this stage can be rotated around the vertical axis within a range of  $\pm 3^\circ$  in a horizontal plane by manually adjusting screws in order to adjust the goniometer surface parallel to the incident beam. A general view of the goniometer is shown in Figure 1.

The drive of the goniometer and X-ray detection system were controlled by a mini-computer (NEC PC-9801E). The program developed by Nomura [5] in MS-Fortran and Macro Assembler languages was modified for the present AXS measurements. The incident beam was monitored by an  $\text{N}_2$  gas ion chamber placed in front of the sample, and the scattering intensity from the sample was measured at each angle for certain preset counts of this ion chamber in order to keep constant the total number of photons hitting the sample. The fluorescent radiation from the sample, mainly arising from the tail of the band pass, and the higher harmonic diffraction of the monochromator crystal is not negligible, particularly at higher angles, even if an energy below the absorption edge is used for the measurements like in the present case. Thus, the separation of this fluorescent component from the scattered intensity is a crucial point in obtaining sufficient reliability of the AXS measurement [7]. The energy resolution of the Ge solid state detector is good enough to clearly separate the  $\text{K}\alpha$  component from the elastic scattering containing the structural information, but insufficient to obtain the  $\text{K}\beta$  component separately. However, since the intensity ratio  $\text{K}\beta/\text{K}\alpha$  is determined with relative-

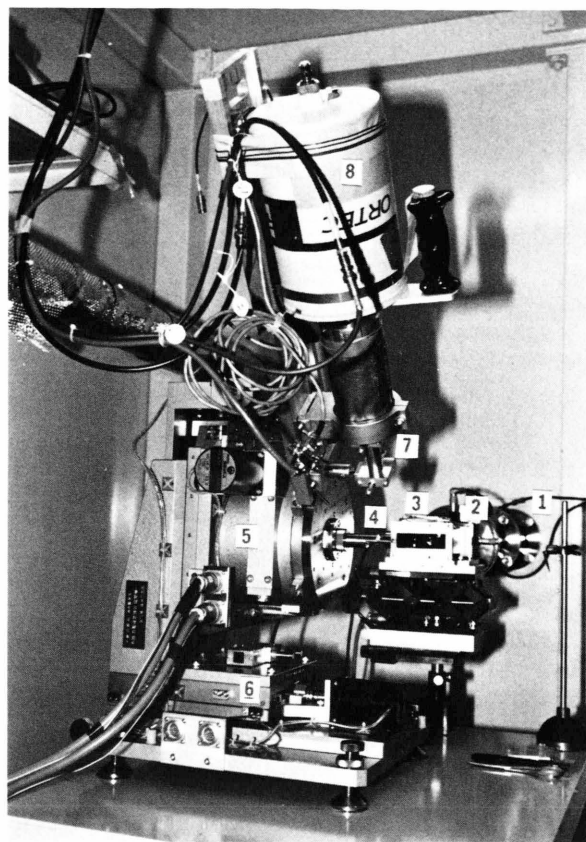


Fig. 1. A general view of a goniometer system newly built at the 7C beam line in the Photon Factory of the National Laboratory for High-Energy Physics, Tsukuba, Japan for exclusive use for the anomalous X-ray scattering (AXS) measurements. 1. beam line; 2. divergent slits; 3. ion chamber; 4. sample; 5. double-axis goniometer; 6. goniometer support table; 7. receiving and scatter slits; 8. pure germanium solid state detector.

ly high accuracy both through the experiment [8, 9] and the theoretical evaluation [10], the intensity of the  $\text{K}\beta$  component can be numerically subtracted in the data reduction process by monitoring the  $\text{K}\alpha$  component. With these careful examinations in mind, the elastic scattering intensity containing the Ge  $\text{K}\beta$  fluorescent component, and Ge  $\text{K}\alpha$  fluorescent radiation were monitored during the present AXS measurements below the Ge  $\text{K}$  absorption edge.

By using the AXS facility shown in Fig. 1, the intensity profiles of the sample were measured at two energies of incidence, i.e. 10.8047 and 11.0795 keV, which respectively correspond to 300 and 25 eV below the Ge  $\text{K}$  absorption edge (11.103 keV). The total intensity measured at the first peak of the scattering profile

of the GeO<sub>2</sub> glass was about 110,000 counts, and at least 50,000 counts were collected even at the angle of minimum intensity. The difference in the intensities at these two energies was about 10% of the intensity at the first peak. The intensity at 11.0795 keV was corrected for the K  $\beta$  component and the escape peak intensity. On the other hand, no Ge fluorescent radiation and escape peak were observed in the measurement at 10.8047 keV. Then, these two intensities were corrected for the absorption by the sample and air in the beam path, and converted to the absolute intensities with the generalized Krogh-Moe-Norman method [11], followed by a correction of the Compton scattering intensity theoretically estimated [12]. Since the energy of the incident beam was selected below the absorption edge in this study, the variation of intensity mainly results from the change of the real part of the anomalous dispersion terms of Ge,  $f'_{\text{Ge}}$  [13]. Thus, the intensity difference in the sample may be given by the equation

$$\begin{aligned} \Delta i(Q) &= I_{300}(Q) - I_{25}(Q) \\ &= c_{\text{Ge}}(f'_{\text{Ge},300} - f'_{\text{Ge},25}) \\ &\quad \cdot \int_0^\infty 4\pi r^2 \sum_{j=1}^2 \text{Re}[f_{j,300}(Q) + f_{j,25}(Q)] \\ &\quad \cdot (\varrho_{\text{Ge}j}(r) - \varrho_{\text{O}j}) \frac{\sin(Qr)}{Qr} dr, \end{aligned} \quad (1)$$

where  $c_{\text{Ge}}$  is the atomic fraction of Ge,  $f_j$  the X-ray atomic scattering factor of the  $j$ th element [14],  $\varrho_{\text{Ge}j}$  the number density function of the  $j$ th atom around a Ge atom, and  $\varrho_{\text{O}j}$  the average number density for  $j$ th element. "Re" indicates the real part of the value in the parentheses. The subscripts 300 and 25 represent the quantities at the energies 10.8047 and 11.0795 keV, respectively. The summation in the above equation indicates the sum over the two constituents in the present sample, that is, germanium and oxygen. The environmental RDF for Ge, which represents the local atomic distribution around a Ge atom, was obtained by the Fourier transformation of the quantity  $Q \Delta i(Q)$ :

$$\begin{aligned} 4\pi r^2 \varrho_{\text{Ge}}(r) &= 4\pi r^2 \varrho_{\text{O}} \\ &\quad + \frac{2r}{\pi} \int_0^\infty \frac{Q \Delta i(Q) \sin(Qr)}{c_{\text{Ge}}(f'_{\text{Ge},300} - f'_{\text{Ge},25}) W(Q)} dQ, \end{aligned} \quad (2)$$

where

$$W(Q) = \sum_{j=1}^2 c_j(f_{j,300}(Q) + f_{j,25}(Q)). \quad (3)$$

$\varrho_{\text{O}}$  in (2) is the average number density of the sample.

A normal X-ray diffraction profile from the sample was also measured using a molybdenum X-ray tube with a singly-bent pyrolytic graphite monochromator in the diffracted beam. A scintillation counter with a pulse-height analyzer was used as a detector. The scattering intensity was collected from at least 20,000 counts for each angle. After the corrections for the absorption and polarization effects along the way similar to the previous works of non-crystalline materials [15, 16], the measured intensity was converted to absolute units, i.e. electron units per atom by the same method used above. Then, from this intensity  $I(Q)$ , the reduced interference function  $i(Q)$  can be obtained,

$$i(Q) = (I(Q) - \langle f^2 \rangle) / \langle f \rangle^2, \quad (4)$$

where  $\langle f \rangle$  is the average atomic scattering factor and  $\langle f^2 \rangle$  the mean square of the atomic scattering factors. By Fourier transformation of the function  $Q i(Q)$ , the ordinary RDF curve is estimated:

$$\begin{aligned} 4\pi r^2 \varrho(r) &= 4\pi r^2 \varrho_{\text{O}} \\ &\quad + \frac{2r}{\pi} \int_0^\infty Q i(Q) \sin(Qr) dQ, \end{aligned} \quad (5)$$

where  $\varrho(r)$  is the so-called average number density distribution function.

## Results and Discussion

The scattering profile from GeO<sub>2</sub> glass by Mo K  $\alpha$  radiation is shown in Figure 2. The experiment was also made on SiO<sub>2</sub> glass for comparison, and the resultant profile given in Fig. 2 is found to agree well with the result of Mozzi and Warren [17]. The profile of the GeO<sub>2</sub> glass shows the typical diffraction pattern of a glass structure. However, the appearance of the profile is quite different from that of the SiO<sub>2</sub> glass. For example, the second and third diffuse peaks at about 26 and 44 nm<sup>-1</sup> are more distinct in the GeO<sub>2</sub> glass although these peaks in the SiO<sub>2</sub> glass are only observed as a small shoulder and a hump, respectively. Figure 3 shows the interference function  $Q i(Q)$  of the GeO<sub>2</sub> glass and makes the difference more conspicuous. This may be explained by the fact that the X-ray atomic scattering factor of a Ge atom is more than two times that of Si. The profile of  $Q i(Q)$  is composed of the first peak at about 15 nm<sup>-1</sup> followed by a number of peaks, which contrasts to the case of metallic

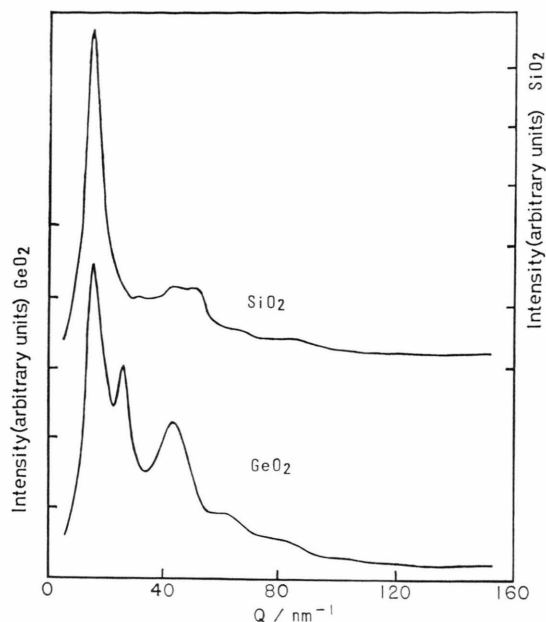


Fig. 2. Diffraction profiles of  $\text{GeO}_2$  and  $\text{SiO}_2$  glasses with Mo K  $\alpha$  radiation.

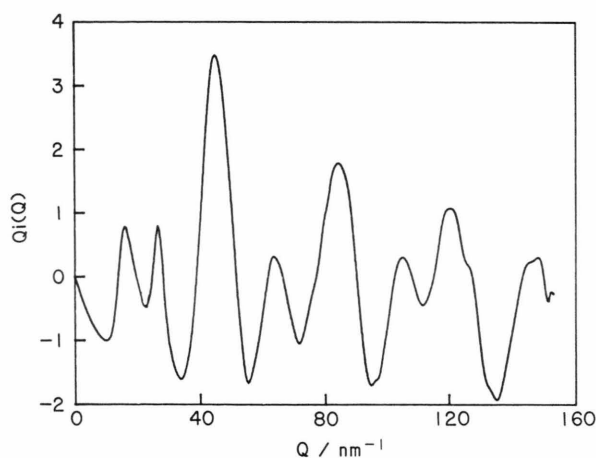


Fig. 3. Interference function  $Qi(Q)$  of  $\text{GeO}_2$  glass.

glasses, where the damping of  $Qi(Q)$  is rapid. If species having definite bond lengths and angles exist in the sample, the oscillations in  $Qi(Q)$  persist in the high  $Q$  region [16, 17]. Therefore, the oscillations observed in the  $\text{GeO}_2$  glass indicate that a considerable fraction of local ordered unit structures exists although their distribution appears to be as random as that of the  $\text{SiO}_4$  tetrahedra observed in  $\text{SiO}_2$  glass.

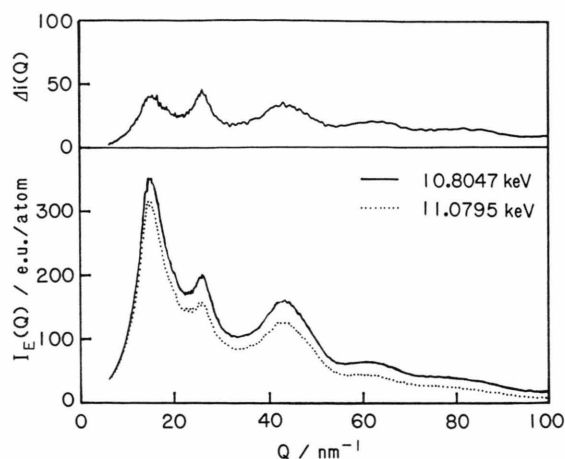


Fig. 4. Differential intensity profile of  $\text{GeO}_2$  glass (top) obtained from the intensity data (bottom) measured at incidence energies of 10.8047 and 11.0795 keV, which correspond to energies 25 and 300 eV below the Ge K absorption edge.

The two scattering intensity profiles at the two energies close to the Ge K absorption edge are shown in Fig. 4, where at the top the differential intensity profile given by (1) is also shown. From this differential curve it is readily found that the intensities of the second and third peaks relatively increase as compared with the intensity of the first peak. Since the atomic correlations around the Ge atoms are emphasized by taking a differential curve at the Ge K edge, we can imagine that the second and third peaks are more strongly attributable to the local atomic configuration around the Ge atoms than the first peak. This may be consistent with the fact that the intensities of the second and third peaks in  $\text{GeO}_2$  glass are much stronger than in  $\text{SiO}_2$  glass.

The environmental interference function  $Q \Delta i(Q)$  computed from the differential curve is shown in Fig. 5, and the environmental RDF curve obtained by Fourier transformation of (2) and the ordinary RDF curve calculated from the interference function  $Qi(Q)$  in Fig. 3 are shown in Fig. 6. Comparing the latter two profiles, it is seen that the peak caused by the correlations of O—O pairs is completely lost in the environmental RDF. This is strong evidence that the present AXS measurement was successfully carried out.

The distances and coordination numbers of the Ge—O, O—O, and Ge—Ge pairs in the ordinary RDF curve were determined by reproducing the experimental RDF curve using the pair correlation func-

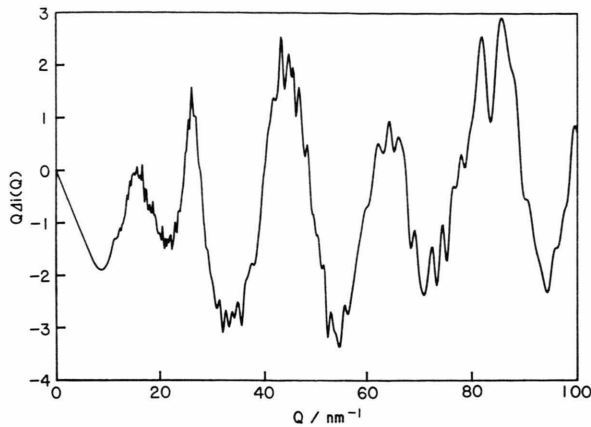


Fig. 5. Differential interference function  $Q \Delta i(Q)$  of GeO<sub>2</sub> for the Ge K absorption edge.

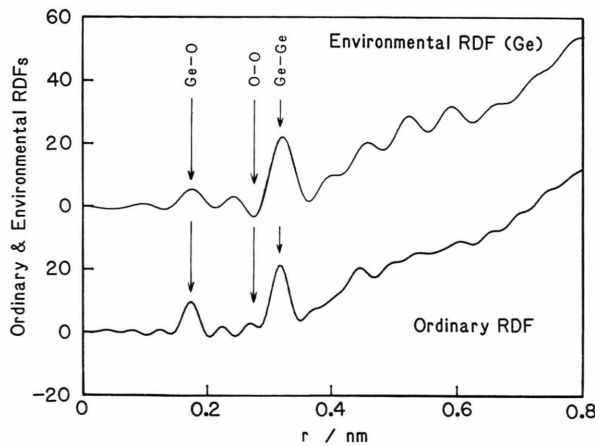


Fig. 6. Environmental radial distribution function (RDF) and ordinary RDF of GeO<sub>2</sub> glass.

Table 1. Comparison of distances  $r_{ij}$  in nm and coordination numbers  $N_{ij}$  of the Ge–O, O–O, and Ge–Ge pairs of GeO<sub>2</sub> glass in the present work with those determined by Lorch [1] with neutrons, by Bondot [3] with Cu K $\alpha$ , Ag K $\alpha$ , and neutrons, and by Sayers *et al.* [20] with EXAFS.

	Ge–O		O–O		Ge–Ge	
	$r_{ij}$	$N_{ij}$	$r_{ij}$	$N_{ij}$	$r_{ij}$	$N_{ij}$
Present Work Mo K $\alpha$	0.173	3.95	0.275	6.4	0.316	4.4
Present Work AXS <sub>Ge</sub>	0.175	4.09 (0.42)			0.320	4.33 (0.20)
Neutrons [1]	0.172	3.8	0.285	–	0.345	–
Cu K $\alpha$ + Ag K $\alpha$ + Neutrons [3]	0.16	–	0.28	–	0.31	–
EXAFS <sub>Ge</sub> [20]	0.174	4			0.315	–

tion method [17, 18]. The peak positions of the Ge–O and Ge–Ge correlations in the environmental RDF were also determined by referring to the ionic radii of germanium and oxygen [19]. The coordination numbers of oxygen and germanium around a germanium were estimated from the area under the corresponding peaks by the following procedure with the assumption that the peak shape is Gaussian: From (2),

$$\begin{aligned}
 4\pi r^2 \varrho_{\text{Ge}}(r) &= 4\pi r^2 \text{Re}[f_{\text{Ge},300}(Q) + f_{\text{Ge},25}(Q)] \varrho_{\text{GeGe}}(r)/W(Q) \\
 &+ 4\pi r^2 \text{Re}[f_{\text{O},300}(Q) + f_{\text{O},25}(Q)] \varrho_{\text{GeO}}(r)/W(Q),
 \end{aligned} \quad (6)$$

where  $\varrho_{\text{GeGe}}(r)$  and  $\varrho_{\text{GeO}}(r)$  are the coordination numbers of Ge and O around Ge. Consequently, the coordination number of Ge or O around Ge is determined by dividing the area by the weighting factor  $\text{Re}[f_{\text{Ge},300}(Q) + f_{\text{Ge},25}(Q)]/W(Q)$  or  $\text{Re}[f_{\text{O},300}(Q) + f_{\text{O},25}(Q)]/W(Q)$ . Since these weighting factors show a weak  $Q$  dependence, the value averaged over the measured  $Q$  region from 7 to 100 nm<sup>−1</sup> was used for estimating the coordination number in the environmental RDF curve. In Table 1 the resultant coordination numbers with their errors due to the variation of this weighting factor are shown together with the distances in both measurements of the present work and those determined by other workers [1, 3]. Sayer *et al.* [20] applied the EXAFS method to a structural study of GeO<sub>2</sub> glass and  $\alpha$ -quartz-type GeO<sub>2</sub> crystals as a reference sample. Table 1 includes their EXAFS results for comparison, although it should be remembered that the theoretical difficulties prevent us to obtain reliable information from the EXAFS signal alone at the present time, particularly for disordered systems with unknown structure as already mentioned by Lee *et al.* [21].

Good agreement is, in the present authors' view, obtained for all distances and coordination numbers of the three pairs in this table, although they were independently determined by completely experimental techniques. The present results clearly indicate that each Ge is surrounded by four oxygens with a Ge–O distance 0.175 nm. Thus it can be concluded that the GeO<sub>4</sub> tetrahedron is quantitatively confirmed as a fundamental local unit structure in the GeO<sub>2</sub> glass. The distance O–O is nearly equal to the edge length of the tetrahedron. Since the number of germanium atoms around a germanium atom is about 4 and the number of O's around O is about 6, each oxygen located at the corner of a tetrahedron is likely to be

bonded with two Ge, so that a network structure formed by the tetrahedra joined at their corners is quite feasible, although a detailed model structure of GeO<sub>2</sub> glass has not yet been established. From the distances Ge–Ge and Ge–O obtained in the present work, the Ge–O–Ge bond angle is also evaluated to be about 132°. Incidentally the bond angle in the  $\alpha$ -quartz type GeO<sub>2</sub> crystal is 130°. Therefore the packing of the GeO<sub>2</sub> tetrahedra might be very similar

to that found in the crystalline modification of GeO<sub>2</sub> as seen in the structural model of SiO<sub>2</sub> glass [17].

Part of this research was supported by the Mitsubishi Foundation research project of anomalous X-ray scattering. We (EM and YW) particularly want to thank the staff of the Photon Factory, National Laboratory for High Energy Physics, Drs. T. Ishikawa and M. Nomura and Profs. T. Matsushita, H. Iwasaki, and M. Ando.

- [1] E. Lorch, *J. Phys. C* **2**, 229 (1969).
- [2] R. N. Sinclair, D. A. Johnson, J. C. Dore, J. H. Clarke, and A. C. Wright, *Nucl. Instrum. Meth.* **117**, 445 (1974).
- [3] P. P. Bondot, *Acta Cryst. A* **30**, 470 (1974).
- [4] C. J. Sparks, G. E. Ice, J. Wong, and B. W. Batterman, *Nucl. Instrum. Methods* **194**, 73 (1982).
- [5] M. Nomura, KEK Report Internal, No. 87-1, (1987).
- [6] T. Ishikawa, J. Matsui, and T. Kitano, *Nucl. Instrum. Methods A* **246**, 613 (1986).
- [7] S. Aur, D. Kofalt, Y. Waseda, T. Egami, R. Wang, H. S. Chen, and B. K. Teo, *Solid State Commun.* **48**, 111 (1983).
- [8] J. H. Williams, *Phys. Rev.* **44**, 146 (1933).
- [9] N. Venkateswara Rao, S. Bhuloka Reddy, G. Satyanarayana, and D. L. Sastry, *Physica* **138 C**, 215 (1986).
- [10] J. H. Scofield, *Atomic Data and Nuclear Data Tables* **14**, 121 (1974).
- [11] C. N. J. Wagner, H. Ocken, and M. L. Joshi, *Z. Naturforsch.* **20a**, 325 (1965).
- [12] D. T. Cromer and J. B. Mann, *J. Chem. Phys.* **47**, 1892 (1967).
- [13] Y. Waseda, *Novel Application of Anomalous X-ray Scattering for Structural Characterization of Disordered Materials*, Springer-Verlag, New York 1984.
- [14] *International Tables for X-ray Crystallography*, Vol. IV, The Knoch Press, Birmingham 1974.
- [15] C. N. J. Wagner, *J. Non-Cryst. Solids* **31**, 1 (1978).
- [16] Y. Waseda, *The Structure of Non-Crystalline Materials*, McGraw-Hill, New York 1980.
- [17] R. L. Mozzi and B. E. Warren, *J. Appl. Cryst.* **2**, 164 (1969).
- [18] E. Matsubara, T. Kawazoe, Y. Waseda, M. Ashizuka, and E. Ishida, *J. Mat. Sci.* **22**, (1987), in press.
- [19] L. Pauling, *The Nature of the Chemical Bond*, 3rd. Ed., Cornell University Press, Ithaca, 1960.
- [20] D. E. Sayers, E. A. Stern, and F. W. Lytle, *Phys. Rev. Lett.* **35**, 584 (1975).
- [21] P. A. Lee, P. H. Citrin, P. Eisenberger, and B. M. Kencaid, *Rev. Mod. Phys.* **53**, 769 (1981).